Liquid Crystals
Publication details, including instructions for authors and subscription information:
http://www.informaworld.com/smpp/title~content=t713926090

Aromatic liquid crystals with a trifluoromethyl group in the terminal chain for use in nematic LC mixtures

G. W. Skelton; J. C. Jones; S. M. Kelly; V. Minter; R. P. Tuffin

To cite this Article Skelton, G. W. , Jones, J. C. , Kelly, S. M. , Minter, V. and Tuffin, R. P.(2001) 'Aromatic liquid crystals with a trifluoromethyl group in the terminal chain for use in nematic LC mixtures', Liquid Crystals, 28: 5, 749 — 759
To link to this Article: DOI: 10.1080/02678290010025486
URL: http://dx.doi.org/10.1080/02678290010025486

LIQUID CRYSTALS, 2001, VOL. 28, NO. 5, 749–759

Aromatic liquid crystals with a trifluoromethyl group in the terminal chain for use in nematic LC mixtures

G. W. SKELTON, J. C. JONES†, S. M. KELLY*, V. MINTER†
and R. P. TUFFIN†
The Department of Chemistry, Hull University, Hull HU6 7RX, UK
†The Defence Evaluation and Research Agency, Malvern WR14 3PS, UK

(*Received 3 August 2000; in final form 9 October 2000; accepted 31 October 2000*)

A new class of compounds suitable for LCD applications has have synthesized, incorporating a trifluoromethyl group in the terminal alkoxy or alkenyloxy chain. These compounds fulfil many of the specifications for use in TN-LCDs. Compounds containing several aromatic rings were synthesized with a view to producing compounds of high birefringence. This aspect also included the synthesis of compounds containing a carbon–carbon triple bond. Materials with three phenyl rings were also prepared in an attempt to produce nematic liquid crystals with a high clearing point and a high birefringence. Molecules containing a lateral fluoro substituent were synthesized in order to generate a high positive value of the dielectric anisotropy, a low melting point and no smectic mesophases. A series of compounds incorporating a carbon–carbon double bond was prepared in an attempt to produce compounds with a high nematic clearing point and a high birefringence.

1. Introduction

Most commercially available liquid crystal displays (LCDs) with high information content utilize the twisted nematic effect (TN-LCDs) [1–12] or in-plane switching (IPS-LCDs) [13–16] with active matrix addressing. These electro-optical effects using nematic liquid crystals can be used to produce large area, light, flat panel displays with a high contrast ratio, grey scale (full colour), fast response times, wide operating temperatures and almost complete absence of cross-talk. The active element at each individual pixel may be a discrete thin film transistor (TFT) [6] or metal–insulator–metal diode (MIM) [7] on an amorphous or crystalline silicon substrate [8]. The TN-LCD requires nematic liquid crystals of high positive dielectric anisotropy in order to produce a low threshold voltage and short response times. Furthermore, they should exhibit a low viscosity and appropriate values of the elastic constants (especially k_{11} and k_{33}) in order to reduce the response times further. A wide operating temperature range requires a low melting point ($T_m < -30$–50°C) and a high clearing point ($T_{N\text{-}I} > 80$–120°C). The birefringence of the mixture is also an important factor. The product of the birefringence and the cell gap (Δnd) is fixed for operation in the first or second transmission minimum [3–5]. Therefore, nematic mixtures of high birefringence enable thin cells to be used. Since both the switch-on and switch-off times are directly proportional to the square of the cell gap, a high birefringence can also give rise to short switching times. The nematic mixtures used in LCDs with active matrix addressing should also exhibit a very high initial value for the resistivity, which should stay as constant as possible over the life-time of the display, in order to maintain the optical performance. A high value for the holding ratio (HR) indicates that the resistivity of the liquid crystal is stable over time.

Nematic liquid crystals containing several halogen atoms, especially fluorine atoms were found to exhibit a stable holding ratio and an acceptable high value of the dielectric anisotropy [17–33]. The value for the permanent dipole moments of several carbon–fluorine bonds were found to be additive, which results in a high value for the dielectric anisotropy. This does not lead to the solvation of ions from the alignment layers, as happens for nematic mixtures of similar dielectric anisotropy incorporating compounds with a cyano group. This is probably due to the low dipole moment of the fluorine–carbon bond and the spatial distribution of the fluorine atoms in polyfluorinated nematic liquid crystals. However, the nematic clearing point of such compounds, especially with two rings, is often low. Thus, corresponding materials with three rings have to be used in relatively high concentrations in order to achieve the desired value of the clearing point. This can give rise to a relatively high viscosity and, consequently, long response times.

---

*Author for correspondence;
e-mail: s.m.kelly@chem.hull.ac.uk

Liquid Crystals ISSN 0267-8292 print/ISSN 1366-5855 online © 2001 Taylor & Francis Ltd
http://www.tandf.co.uk/journals
DOI: 10.1080/02678290010025486

We have synthesized a new class of compounds suitable for LCD applications, incorporating a trifluoromethyl group situated at the end of a terminal alkoxy or alkenyloxy chain. These aromatic compounds fulfil many of the specifications for use in TN-LCDs, including that of possessing high birefringence. These materials were designed so that the resultant dipole moment due to three carbon–fluorine bonds at the same carbon atom is as parallel as possible to the molecular long axis, i.e. the nematic director, see figure 1. Although the 4,4,4-trifluorobutyloxy chain chosen for initial study may adopt non-linear conformations (which would reduce the component of the dipole moment parallel to the director), this is not possible for the (*E*)-4,4,4-trifluorobut-2-enyloxy chain, see figure 2. A comparison of the experimentally determined dipole moment of compounds containing these two groups should give some indication of the conformation of these chains in the nematic phase. The presence of a carbon–carbon double bond in an appropriate position and configuration is known to promote the formation of the nematic phase and contribute to a high birefringence.

2. Synthesis

The ethers **1–22** were prepared from the appropriate alkyl bromide or tosylate and a range of phenols via the Williamson ether synthesis, as indicated below. The aryl 4,4,4-trifluorobutyl ethers **1–3**, **7** and **13–16** and (*E*)-4,4,4-trifluorobut-2-enyl ethers **4–6**, **8**, **17–19** and **22** were synthesized by the reaction of the appropriate phenol with commercially available 1-bromo-4,4,4-trifluorobutane or toluene-4-sulphonic acid (*E*)-4,4,4-trifluorobutenyl ester. This tosylate was produced in the normal way from (*E*)-4,4,4-trifluorobut-2-en-1-ol and 4-methylbenzenesulphonyl chloride [34]. The corresponding non-fluorinated butyloxy compounds **9** and **20** and the (*E*)-but-2-enyloxy materials **10** and **21**, synthesized for comparison purposes, were prepared in a similar fashion using commercially available 1-bromobutane or (*E*)-1-chloro-but-2-ene and the appropriate phenol. The 4-*n*-alkyl-4′-hydroxybiphenyls were commercially available. 3-Fluoro-4-hydroxy-4′-heptylbiphenyl was prepared by the aryl–aryl cross coupling [35] of 1-bromo-4-heptylbenzene and 4-benzyloxy-3-fluorophenylboronic acid in a Suzuki reaction [36] yielding 4-benzyloxy-3-fluoro-4′-heptylbiphenyl which was then deprotected by catalytic hydrogenolysis. The corresponding 4-*n*-alkyl-4′-hydroxytolanes with an additional carbon–carbon triple bond were prepared by cross coupling commercially available 4-*n*-alkylacetylenes with 4-iodophenol using a palladium catalyst [37]. The synthesis of the other, non-commercially available phenols, was carried out as recently described [38].

3. Phase characterization

3.1. *Phase characterization by thermal optical microscopy*

The thermotropic mesophases observed for the compounds shown in tables 1–4 were investigated using polarizing optical microscopy (POM). The only phases observed were smectic phases including the smectic A

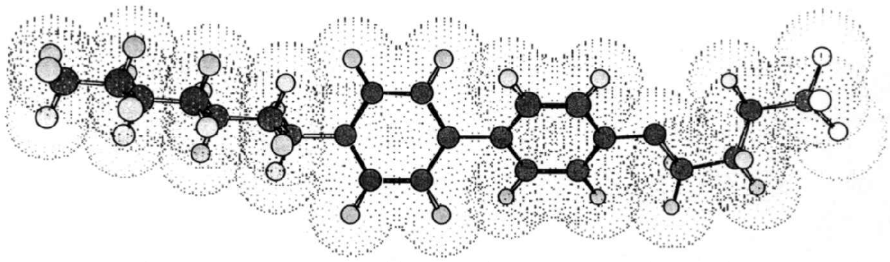

Figure 1. The energy-minimized structure of 4-heptyl-4′-(4,4,4-trifluorobutyloxy)biphenyl (**3**) calculated using MOPAC with AM1 theory and a closed shell (restricted) wave function.

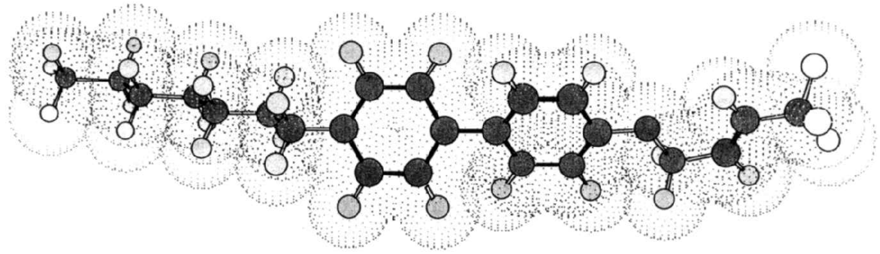

Figure 2. The energy-minimized structure of 4-heptyl-4′-[(*E*)-4,4,4-trifluorobut-2-enyloxy]biphenyl (**6**) calculated using MOPAC with AM1 theory and a closed shell (restricted) wave function.

Table 1. Transition temperatures (°C) and some enthalpies of transition ($J\ g^{-1}$) for 4-*n*-alkyl-4′-(4,4,4-trifluorobutyloxy)biphenyls (**1–3**), 4-*n*-alkyl-4′-[(*E*)-4,4,4-trifluorobut-2-enyloxy]biphenyls (**4–6**), 3′-fluoro-4-heptyl-4′-(4,4,4-trifluorobutyloxy)biphenyl (**7**), 3′-fluoro-4-heptyl-4′-[(*E*)-4,4,4-trifluorobut-2-enyloxy]biphenyl (**8**), 4-butyloxy-4′-pentylbiphenyl (**9**) and 4-[(*E*)-but-2-enyloxy]-4′-pentylbiphenyl (**10**).

Compound	Structure	Cr	SmX	SmB	SmA	N	I
1	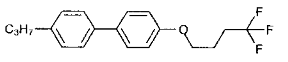	● 97 (27.6)	[a](● 93)† (5.9)	● 108 (6.2)	● 116 (25.6)	—	●
2	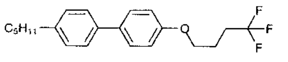	● 63 (34.8)	(● 54)† (3.4)	● 99 (6.5)	● 103 (19.1)	[b][● 63]#	●
3	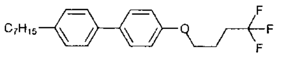	● 29 (12.9)	● 40 (2.3)	● 98 (31.1)	—	[● 63]	●
4	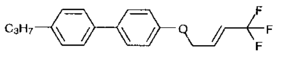	● <25	● 106 (8.2)	—	● 137 (57.8)	—	●
5	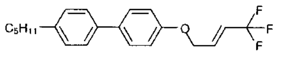	● 66 (15.5)	● 116 (4.1)	—	● 121 (25.8)	[● 53]#	●
6	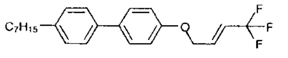	● <25	● 107 (4.6)	—	● 117 (40.0)	—	●
7	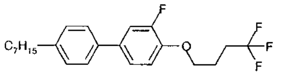	● 56	—	—	(● 52)†	[● −5]#	●
8	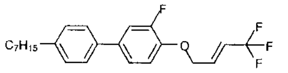	● 64	—	(● 60)†	(● 63)†	[● 20]#	●
9	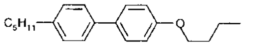	● 63	—	● 89	—	[● 48]#	●
10	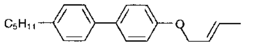	● 75 (17.4)	—	● 103 (25.8)	—	[● 48]#	●

[a] ()† Represents a monotropic transition temperature.
[b] []# Represents an extrapolated transition temperature.

phase (SmA), the smectic B phase (SmB) and an unidentified, ordered smectic phase (SmX). The focal-conic (fan) texture was always observed on cooling from the isotropic liquid to form the smectic A phase, along with optically extinct homeotropic areas. As the sample was cooled further the texture often formed more optically extinct homeotropic areas, indicating that the phase is optically uniaxial. The simultaneous presence of both homeotropic and focal-conic textures, confirms that the mesophase observed is indeed a calamitic smectic A phase. The dark elliptical and hyperbolic lines of optical discontinuity characteristic of focal-conic defects were also observed. This optical behaviour is consistent with the mesophase being smectic A with a layered structure, with the long axes of the molecules lying on average orthogonal to the layer planes, and the in-plane and out-of-plane positional ordering of the molecules being short range.

On cooling the smectic A phase, several of the compounds exhibited dark transition bars across the backs of the focal-conics over a short temperature range. This transitory behaviour was also observed on heating. The homeotropic areas did not change in appearance. This behaviour is characteristic of a transition between a SmB phase and a SmA phase. It is not possible to determine with any certainty whether a hexatic SmB phases or a crystal SmB phase is observed in the absence of X-ray studies. In a few cases the SmB phase was formed directly from the isotropic liquid. A mosaic texture was observed after the initial formation of H-shaped patterns from the nematic phase. These coalesced quickly to form a multicoloured mosaic texture. The smectic X phase, which also exhibited a mosaic texture, could not be identified with any degree of certainty by optical microscopy in the absence of X-ray investigations. It is almost certainly a tilted crystal smectic phase.

An extrapolated 'virtual' value for the nematic–isotropic transition temperature was determined in order to evaluate the use of these materials in nematic mixtures. A linear clearing point relationship across the phase diagram was assumed for mixtures of different composition of the test material in the commercial nematic mixture E7. Linear extrapolation of the transition temperature line to 100% of the test material gave the value

Table 2. Transition temperatures (°C) and some enthalpies of transition (J g^{-1}) for 4-pentyl-4′-trifluoromethoxybiphenyl (**11**) [30], 4-pentyl-4′-(2,2,2-trifluoroethoxy)biphenyl [**12**) [31], 4-pentyl-4′-(4,4,4-trifluorobutyloxy)biphenyl (**2**), 4-pentyl-4″-(4,4,4-trifluorobutyloxy)terphenyl (**13**), 4-*n*-alkyl-4′-(4,4,4-trifluorobutyloxy)tolanes (**14–16**) and 4-*n*-alkyl-4′-[(*E*)-4,4,4-trifluorobut-2-enyloxy]-tolanes (**17–19**).

Compound	Structure	Cr	SmX	SmB	SmA	N	I
11	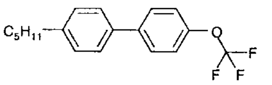	• 67	—	—	—	—	•
12	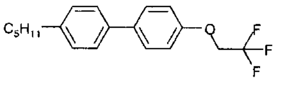	• 107	—	—	—	[b][• −30]#	•
2	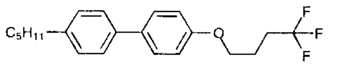	• 63	—	• 99	• 103	[• 63]#	•
13	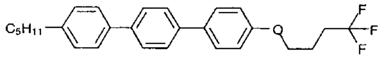	• 203	—	—	• 267	—	•
14	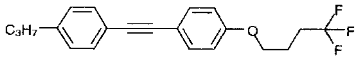	• 106 (72.5)	—	—	—	[• 83]#	•
15	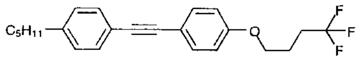	• 98 (62.7)	[a](• 86)† (21.0)	—	—	[• 85]#	•
16	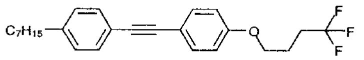	• 76 (35.7)	• 91 (24.5)	—	—	[• 85]#	•
17	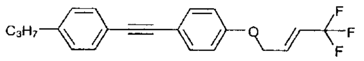	• 130 (59.9)	—	—	—	[• 67]#	•
18	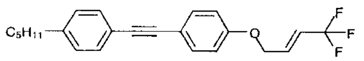	• 106 (34.5)	• 120 (37.7)	—	—	[• 74]#	•
19	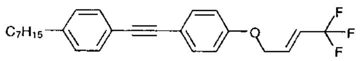	• 87 (31.1)	• 121 (37.8)	—	—	[• 76]#	•

[a] ()† Represents a monotropic transition temperature.
[b] []# Represents an extrapolated transition temperature.

Table 3. Transition temperatures (°C) and some enthalpies of transition (J g^{-1}) for 4-butyloxy-4″-pentylterphenyl (**20**), 4-[(*E*)-but-2-enyloxy]-4″-pentylterphenyl (**21**), 4-pentyl-4″-(4,4,4-trifluorobutyloxy)terphenyl (**13**) and 4-pentyl-4″-[(*E*)-4,4,4-trifluorobut-2-enyloxy]terphenyl (**22**).

Compound	Structure	Cr	SmB	SmA	I
20	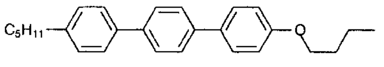	• 125 (12.3)	• 220 (8.5)	• 240	•
21	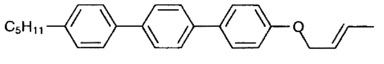	• 70 (21.3)	• 207	• 220	•
13	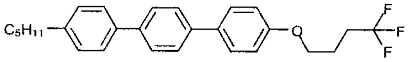	• 203	—	• 267	•
22	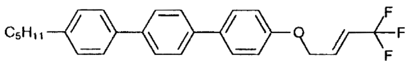	• 239 (7.1)	• 245 (7.1)	• 270 (30.2)	•

of the extrapolated nematic clearing point. The extrapolation was made over as short a composition range as possible in order to be as certain as possible that no curvature of the line occurs.

3.2. *Phase characterization by differential scanning calorimetry*

Enthalpy values for the liquid crystal transitions for some of the compounds prepared are collated in

Table 4. Dipole moments (D) and $T_{\mathrm{N\text{-}I}}$(°C) for 4-heptyl-4′-(4,4,4-trifluorobutyloxy)biphenyl (**3**), 4-heptyl-4′-[(*E*)-4,4,4-trifluorobut-2-enyloxy]biphenyl (**6**), 3′-fluoro-4-heptyl-4′-(4,4,4-trifluorobutyloxy)biphenyl (**7**) and 3′-fluoro-4-heptyl-4′-[(*E*)-4,4,4-trifluorobut-2-enyloxy]biphenyl (**8**).

Compound	Structure	μ	T_{NI}
3	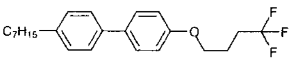	9.7	^{a}[63]$^{\#}$
6	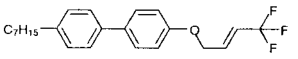	15.4	[48]$^{\#}$
7	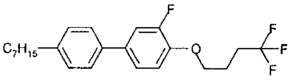	17.8	[− 5]$^{\#}$
8	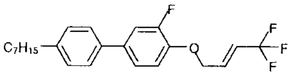	18.2	[20]$^{\#}$

^{a} []$^{\#}$ Represents an extrapolated transition temperature.

tables 1–3 (shown in brackets). The enthalpy of fusion (22.8–71.4 J g^{-1}) and the enthalpy of transition from the lamellar smectic A and B phases to the disordered isotropic phase (19.1–57.8 J g^{-1}) are large as expected. The enthalpy of transition between the SmB and the SmX phase varies significantly from compound to compound (6.2–31.0 J g^{-1}). The lower values observed for some of these transitions may indicate that the SmB phase is a highly ordered crystal B phase. The values measured, which were determined twice on heating and cooling cycles on the same sample, are of a normal magnitude for liquid crystals. The value determined on the first heating cycle is quoted in the tables. However, the values obtained on separate samples of the same compounds were reproducible and very little thermal degradation of the sample was observed. A typical heating thermogram is shown in figure 3 for compound **1**. The base line is always relatively flat and sharp transition peaks are observed. The values for the transition temperatures agree well (≈ 1–2°C) with those values determined by optical microscopy. A melting point could not be determined for several compounds with a smectic X phase due to the highly crystalline nature of this phase. The high enthalpy change associated with the transition from an ordered smectic phase to the isotropic liquid is shown in figure 4 for compound **18**.

4. Mesomorphism

The thermal data for a series of compounds **1–12** with three fluorine atoms in a terminal position of an alkenyl or alkenyloxy chain are collated in table 1. The ethers **1–3** all exhibit smectic liquid crystalline phases. However, compounds **1** and **2** exhibit a SmB phase, a SmA phase and a monotropic, unidentified ordered smectic phase, whereas compound **3** shows only an ordered smectic phase and a SmB phase. As the alkyl chain length increases, the clearing point and the transition temperature for the ordered smectic phase decrease, while the SmB phase transition temperature remains relatively stable. Therefore, the temperature range of the SmA phase decreases as the alkyl chain length increases. However, preliminary results for compound **2**, which possesses a high extrapolated ‘virtual’ nematic clearing point (63°C),

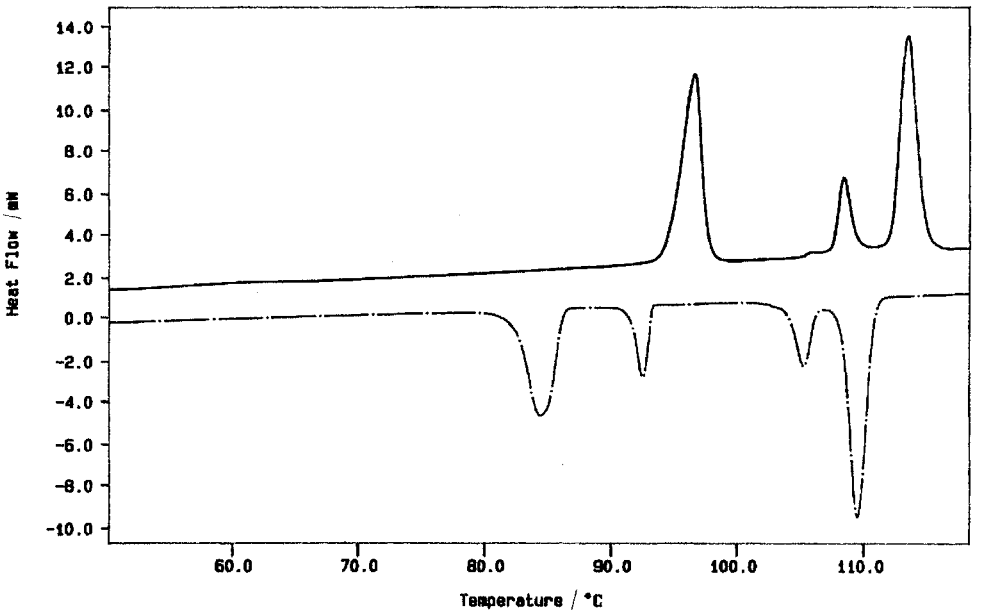

Figure 3. Differential scanning thermograms for the first heating (full line) and cooling cycles for 4-pentyl-4′-(4,4,4-trifluorobutyloxy)-biphenyl (**1**); scan rate 10°C min^{-1}.

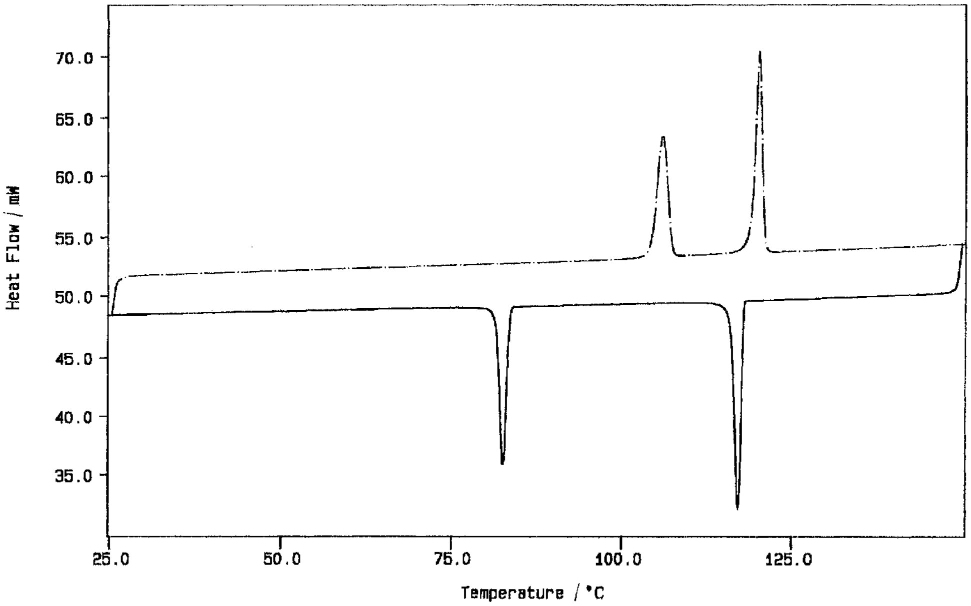

Figure 4. Differential scanning thermogram as a function of temperature for the first heating (full line) and cooling cycles for 4-pentyl-(4,4,4-trifluorobutyloxy)tolane (**18**); scan rate 10°C min^{-1}.

indicate that these compounds may be useful as components of a nematic mixture, despite the absence of an enantiotropic nematic phase for the compounds themselves—see below.

The (*E*)-4,4,4-trifluorobut-2-enyloxy substituted ethers **4–6** contain a *trans*-carbon–carbon double bond in the terminal chain. The presence of the double bond increases the clearing point (20°C, on average) compared with that of the corresponding 4,4,4-trifluorobutyloxy ethers **1–3**. The presence of the double bond also increases the tendency to form more ordered smectic phases, all of the compounds exhibiting an ordered smectic phase and a SmB phase, but no SmA phase. The *trans*-carbon–carbon bond eliminates non-linear conformations in the terminal (*E*)-trifluorobut-2-enyloxy chain. This may induce a more orderly arrangement of the molecules within the smectic layers. The presence of the *trans*-carbon–carbon double bond does not produce an observable nematic phase or reduce the smectic transition temperatures or the tendency for smectic phase formation. This is inconsistent with the usual effect of the presence of a carbon–carbon double bond on the liquid crystal compound containing it [2, 39, 40].

The two compounds **3** and **7** are almost identical, except for the presence of a lateral fluoro-substituent in compound **7** in place of a hydrogen atom. Compound **3** exhibits an ordered smectic phase and a SmB phase and has an extrapolated nematic–isotropic transition temperature above room temperature (63°C). Compound **7** exhibits only a monotropic smectic A phase (52°C). In addition, the extrapolated nematic clearing point of compound **7** is low (– 5°C). This is clearly attributable to the steric effect of the fluorine atom in a lateral position, which increases the intermolecular separation. This should lead to less ordered smectic phases at lower temperatures, as is indeed observed to be the case for the compounds studied here. The transition temperatures for the (*E*)-4,4,4-trifluorobut-2-enyloxy compounds **6** and **8** are higher than those of the analogous 4,4,4-trifluorobut-2-enyloxy compounds **3** and **7**, with the exception of the melting point of compound **6**. Compound **8**, containing a fluorine atom in a lateral position, has lower transition temperatures. The double bond in compound **8** also induces an ordered SmB phase, which compound **7** does not display. The liquid crystal transition temperatures of the (*E*)-4,4,4-trifluorobut-2-enyloxy compounds **6** and **8**, compared with those of the analogous 4,4,4-trifluorobutyloxy compounds **3** and **7**, are probably attributable to the presence of the *trans*-carbon–carbon double bond. The extrapolated nematic–isotropic transition temperature for compounds **6** and **8** are higher than those of the corresponding compounds **3** and **7** without a carbon–carbon double bond, as expected [2, 39, 40].

Compound **9** exhibits only a SmB phase. The presence of a trifluoromethyl group at the end of the terminal chain of compound **2** induces a smectic A phase and a higher clearing point (+ 14°C) than that of compound **9**. Additionally, its extrapolated nematic clearing point is higher (+ 15°C) than that of the analogous butyloxy compound **9**. Compound **5** exhibits a SmX and a SmA phase, whereas the analogous compound **10** possesses only a SmB phase. The transition temperatures are, however, higher than those of compounds **2** and **9**, with the exception of the extrapolated nematic clearing point for compound **10**. It is interesting to note that the presence of a *trans*-carbon–carbon double bond in compound **5** and **10** leads to higher transition temperatures for the melting point and the smectic phases than those of compound **2** and **9**, respectively. Surprisingly, the value for the extrapolated clearing point of compound **5** is lower than that of compound **2**.

Table 2 shows first a comparison of the liquid crystal transition temperatures of compounds **2**, **11** and **12**, which differ only in the length of their ω,ω,ω-trifluoroalkoxy chain. As pure compounds, **11** and **12** are not liquid crystalline. Compound **12** does, however, give an extrapolated nematic clearing point below room temperature (– 30°C). Compound **2** exhibits an enantiotropic SmB phase and a SmA phase. The extrapolated nematic–isotropic transition temperature of compound **2** is also much higher than that of compound **12**. The transition temperatures of the terphenyl **13** are, as expected, much higher than those of the corresponding biphenyl homologue **2**. In addition to this, compound **13** displays only a smectic A phase with a wide temperature range (64°C). The clearing point of the terphenyl **13** is much higher (+ 150°C) than that of compound **2**, which also exhibits a SmB phase. Compound **13** was too insoluble in a nematic host mixture to allow an extrapolated nematic clearing point to be obtained.

Table 2 also contains thermal data for three homologues of 4,4,4-trifluorobutyloxy substituted tolanes **14–16** and (*E*)-4,4,4-trifluorobut-2-enyloxy substituted tolanes **17–19**. Compound **14** is not mesomorphic. Compound **15** exhibits a monotropic ordered smectic phase, and compound **16** possesses the enantiotropic ordered smectic phase, which is now enantiotropic. Although the clearing point decreases as the alkyl chain length increases, the extrapolated nematic–isotropic transition temperature is remarkably similar for all three homologues. Compound **15** displays only a monotropic ordered smectic phase. The extrapolated virtual nematic–isotropic transition temperature of the tolane **15** is much higher than that of the analogous biphenyl **2**. This is almost certainly due to the greater length-to-breadth ratio of the tolane and the greater degree of anisotropy of the molecular polarisability. The tendency to form the SmX phase increases with increasing chain length. The (*E*)-4,4,4-trifluorobut-2-enyloxy compounds **17–19** exhibit higher transition temperatures than the analogous 4,4,4-trifluorobutyloxy compounds **14–16**. The propyl homologue **17** is not liquid crystalline. Compounds **18** and **19** exhibit an ordered smectic phase. The extrapolated virtual nematic clearing points of the (*E*)-4,4,4-trifluorobut-2-enyloxy compounds **17–19** are lower (12°C, on average) than those for the analogous 4,4,4-trifluorobutyloxy compounds **14–16**. This is very unusual and may, perhaps, be attributable, at least in part, to uncertainties in the extrapolation procedure.

The thermal data for the pentyl homologue of four related terphenyl compounds, differing only in the presence of three fluorine atoms or a *trans*-carbon–carbon double bond, are collated in table 3. The non-fluorinated compounds **20** and **21** exhibit a SmB phase and a SmA phase. Compound **21** has much lower melting and clearing points as well as a narrower SmA phase than compound **20**. In contrast, compounds **13** and **22**, incorporating three fluorine atoms in a terminal position, possess higher transition temperatures. Compound **13** displays only a SmA phase; however, the high melting point prohibits any other phases from being observed. The presence of a *trans*-carbon–carbon double bond in compound **22** produces even higher transition temperatures. It is interesting to note that compared with compound **13**, compound **22** displays an enantiotropic SmB phase.

5. Dipole moments

Data for the dipole moments and the extrapolated nematic–isotropic transition temperatures for compounds **3** and **6–8** are collated in table 4. Molecular modelling using the commercial Cerius^2 package on a Sun Workstation suggests that the dipole moment of the trifluoromethyl group at the end of the terminal chain of the ethers **3** and **6–8** is almost parallel to the molecular long axis, see also figure 1. This appears to be confirmed by the data in table 4, showing large dipole moments for these materials. Compound **7** confirms that the inclusion of a fluorine atom in a lateral position greatly increases the dipole moment. Unfortunately, a consequence of the incorporation of such a lateral fluorine is a much lower clearing point, i.e. the extrapolated nematic–isotropic transition temperature for compound **7** is below room temperature. These effects are often additive for polyfluorinated compounds [25–31]. Interestingly, the inclusion of a *trans*-carbon–carbon double bond into the core system **6** increases the dipole almost to the same extent as the inclusion of a lateral fluorine substituent. This may be attributable to the absence of non-linear conformations for this terminal unit, see figure 2. This is consistent with the high value for the extrapolated nematic clearing point. Therefore, it is not surprising that compound **8**, which combines a *trans*-carbon–carbon double bond and a fluorine atom in a lateral position *ortho* to the (*E*)-4,4,4-trifluorobut-2-enyloxy chain, should possess the highest dipole moment of the four compounds. The presence of a *trans*-carbon–carbon double bond in compound **8** also increases its virtual nematic clearing point relative to that of compound **7**.

6. Experimental

6.1. *Characterization*

The structures of all intermediates and final products were confirmed by proton (^{1}H) nuclear magnetic resonance (NMR) spectroscopy (JOEL JMN-GX270 FT nuclear resonance spectrometer), infra-red (IR) spectroscopy (Perkin Elmer 783 infra-red spectrophotometer) and mass spectrometry (MS) (Finnegan MAT 1020 automated GC/MS). Reaction progress and product purity were checked using a CHROMPACK CP 9001 capillary gas chromatograph fitted with a 10 m CP-SIL 5CB (0.12 μm, 0.25 mm) capillary column. Transition temperatures were determined using an Olympus BH-2 polarizing light microscope together with a Mettler FP52 heating stage and a Mettler FP5 temperature control unit. The analysis of transition temperatures and enthalpies was carried out by a Perkin-Elmer DSC7-PC differential scanning calorimeter.

Tetrahydrofuran was dried by distillation over sodium wire and in the presence of benzophenone and then stored over 4 Å molecular sieves. Diethyl ether was dried and stored over sodium wire. Pyridine and triethylamine were distilled over potassium hydroxide pellets and then stored over 5 Å molecular sieves. Dichloromethane was dried by distillation over phosphorus pentoxide. Chloroform was alumina-filtered to remove residual ethanol.

6.2. *General synthetic procedures*

6.2.1. *4-Benzyloxy-3-fluoro-4′-heptylbiphenyl*

A mixture of 1-bromo-4-heptylbenzene (7.26 g, 28.46 mmol), 4-benzyloxy-3-fluorophenylboronic acid (7.00 g, 28.46 mmol) and tetrakis(triphenylphosphine)-palladium(0) (0.50 g), 2M sodium carbonate solution (140 cm^3) and 1,2-dimethoxy methane (200 cm^3) was heated under reflux (80°C) overnight. The reaction mixture was added to water (200 cm^3), the organic layer separated off and the aqueous layer shaken with dichloromethane (3×50 cm^3). The combined organic layers were washed with dilute sodium carbonate solution (2×100 cm^3), dried ($MgSO_4$), filtered and the solvent removed. The resultant crude product was then recrystallized from ethanol (5.25 g, 49%). SmB–SmA, 194°C; SmA–N, 206°C; N–I, 218°C; purity 98.4%. ^{1}H NMR ($CDCl_3$) δ: 0.89 (3H, t), 1.31 (8H, m), 1.64 (2H, m), 2.63 (2H, t), 5.02 (2H, s), 7.04 (1H, m), 7.24 (4H, m), 7.42 (7H, m). IR (KBr)ν_{max}/cm^{-1}: 2920, 1620, 1500, 1270, 1130, 1000, 820, 740, 710. MS *m*/*z*: 376 (M^+), 285, 91.

6.2.2. *3-Fluoro-4′-heptyl-4-hydroxybiphenyl*

10% Palladium-on-charcoal (0.5 g) was added to 4-benzyloxy-3-fluoro-4′-heptylbiphenyl (3.90 g, 10.37 mmol) in terahydrofuran (250 cm^3) and ethanol (30 cm^3). The mixture was then stirred under hydrogen. When GC analysis suggested the reaction was complete, the catalyst was filtered off, the solvent removed under reduced pressure and the crude solid product recrystallized from ethanol (2.49 g, 84%). Cr–I, 209°C; purity 98.9%. ^{1}H NMR ($CDCl_3$) δ: 0.88 (3H, t), 1.31 (8H, m), 1.63 (2H, m), 2.62 (2H, t), 5.03 (1H, s), 7.04 (1H, m), 7.24 (4H, m), 7.44 (2H, m). IR (KBr)ν_{max}/cm^{-1}: 3400, 2920, 1600, 1500, 1400, 1170, 1000, 810. MS *m*/*z*: 286 (M^+), 201, 58.

6.2.3. *4-Hydroxy-4′-propyltolane*

4-Propylphenylacetylene (5.00 g, 34.72 mmol) was added dropwise with stirring to a mixture of 4-iodophenol (7.28 g, 33.67 mmol), $Pd(PPh_3)_2Cl_2$ (0.46 g, 0.66 mmol), copper(I) iodide (0.25 g, 1.32 mmol), triethylamine (5.00 g, 49.60 mmol) and tetrahydrofuran (40 cm^3). The mixture was stirred overnight at room temperature, filtered and the solvent removed under reduced pressure. The crude product was purified by column chromatography on silica gel using a 1 : 1 mixture of light petroleum (b.p. 40–60°C) and dichloromethane as eluent, and recrystallization from hexane to give the desired tolane (4.42 g, 57%); purity 96.2%. ^{1}H NMR ($CDCl_3$) δ: 0.94 (3H, t), 1.65 (2H, sex), 2.59 (2H, t), 4.83 (1H, s), 6.81 (2H, m), 7.14 (2H, m), 7.42 (4H, m). IR (KBr)ν_{max}/cm^{-1}: 3500, 2960, 1600, 1520, 1450, 1250, 1100, 840. MS *m*/*z*: 236 (M^+), 207, 178.

The following tolanes were prepared in a similar way.

6.2.4. *4-Hydroxy-4′-pentyltolane*

Yield 2.84 g, 39%. ^{1}H NMR ($CDCl_3$) δ: 0.89 (3H, t), 1.32 (4H, m), 1.62 (2H, m), 2.61 (2H, t), 4.86 (1H, s), 6.80 (2H, m), 7.15 (2H, m), 7.41 (4H, m). IR (KBr)ν_{max}/cm^{-1}: 3230, 2930, 1600, 1520, 1450, 1250, 1180, 1100, 840. MS *m*/*z*: 264 (M^+), 207, 178.

6.2.5. *4-Heptyl-4′-hydroxytolane*

Yield 1.34 g, 46%. ^{1}H NMR ($CDCl_3$) δ: 0.88 (3H, t), 1.28 (8H, m), 1.61 (2H, m), 2.61 (2H, t), 4.86 (1H, s), 6.81 (2H, m), 7.14 (2H, m), 7.42 (4H, m). IR (KBr)ν_{max}/cm^{-1}: 3330, 2930, 1600, 1520, 1450, 1250, 1180, 1100, 840. MS *m*/*z*: 292 (M^+), 207, 178.

6.2.6. *4-Propyl-4′-(4,4,4-trifluorobutyloxy)biphenyl* (**1**)

A mixture of 1-bromo-4,4,4-trifluorobutane (0.56 g, 2.93 mmol), 4-hydroxy-4′-propylbiphenyl (0.50 g, 2.36 mmol), potassium carbonate (1.30 g, 9.43 mmol) and butanone (40 cm^3) was heated at 80°C overnight. The cooled reaction mixture was filtered and the filtrate evaporated under reduced pressure. The crude product was purified by column chromatography on silica gel using a 95 : 5 (v/v) mixture of light petroleum (b.p. 40–60°C) and ethyl acetate as eluent and recrystallization from ethanol to give the desired ether (0.41 g, 54%). Cr 97°C SmX 108°C SmA 116°C I; purity 99.7%. ^{1}H NMR

($CDCl_3$) δ: 0.98 (3H, t), 1.68 (2H, sex), 2.07 (2H, m), 2.33 (2H, m), 2.62 (2H, t), 4.06 (2H, t), 6.95 (2H, m), 7.24 (2H, m), 7.49 (4H, m). IR (KBr)ν_{max}/cm^{-1}: 2960, 1600, 1490, 1240, 1150, 1030, 800. MS m/z: 322 (M^+), 293, 183.

The following final products were prepared in a similar fashion using the appropriate phenol and alkyl halide or tosylate as described in § 2. The purity of all the final products was greater than 99.7% by GC. Their transition temperatures are recorded in tables 1–4.

6.2.7. *4-Pentyl-4′-(4,4,4-trifluorobutyloxy)biphenyl (**2**)*

^{1}H NMR ($CDCl_3$) δ: 0.90 (3H, t), 1.35 (4H), 1.65 (2H, m), 2.05 (2H, m), 2.35 (2H, m), 2.65 (2H, t), 4.06 (2H, t), 6.95 (2H, m), 7.24 (2H, m), 7.48 (4H, m). IR (KBr)ν_{max}/cm^{-1}: 2920, 1600, 1500, 1450, 1250, 1150, 1030, 800. MS m/z: 350 (M^+), 293, 183.

6.2.8. *4-Heptyl-4′-(4,4,4-trifluorobutyloxy)biphenyl (**3**)*

^{1}H NMR ($CDCl_3$) δ: 0.88 (3H, t), 1.32 (8H, m), 1.64 (2H, m), 2.08 (2H, m), 2.33 (2H, m), 2.63 (2H, t), 4.05 (2H, t), 6.94 (2H, m), 7.23 (2H, m), 7.48 (4H, m). IR (KBr)ν_{max}/cm^{-1}: 2920, 1600, 1490, 1245, 1150, 1030, 810. MS m/z: 378 (M^+), 293, 183.

6.2.9. *4-Propyl-4′-[(E)-4,4,4-trifluorobut-2-enyloxy]-biphenyl (**4**)*

^{1}H NMR ($CDCl_3$) δ: 0.96 (3H, t), 1.68 (2H, sex), 2.61 (2H, t), 4.68 (2H, m), 6.09 (1H, m), 6.59 (1H, m), 6.95 (2H, m), 7.24 (2H, m), 7.50 (4H, m). IR (KBr)ν_{max}/cm^{-1}: 2930, 1600, 1490, 1320, 1240, 1130, 1030, 960, 810. MS m/z: 320 (M^+), 211, 154.

6.2.10. *4-Pentyl-4′-[(E)-4,4,4-trifluorobut-2-enyloxy]-biphenyl (**5**)*

^{1}H NMR ($CDCl_3$) δ: 0.91 (3H, t), 1.36 (4H, m), 1.65 (2H, m), 2.32 (2H, t), 4.69 (2H, m), 6.10 (1H, m), 6.57 (1H, m), 6.97 (2H, m), 7.24 (2H, m), 7.50 (4H, m). IR (KBr)ν_{max}/cm^{-1}: 2940, 1610, 1500, 1450, 1310, 1270, 1130, 960, 810. MS m/z: 348 (M^+), 239, 182.

6.2.11. *4-Heptyl-4′-[(E)-4,4,4-trifluorobut-2-enyloxy]-biphenyl (**6**)*

^{1}H NMR ($CDCl_3$) δ: 0.88 (3H, t), 1.31 (8H, m), 1.63 (2H, m), 2.63 (2H, t), 4.69 (2H, m), 6.09 (1H, m), 6.58 (1H, m), 6.97 (2H, m), 7.23 (2H, m), 7.49 (4H, m). IR (KBr)ν_{max}/cm^{-1}: 2920, 1600, 1500, 1330, 1240, 1130, 1030, 960, 820. MS m/z: 376 (M^+), 267, 154.

6.2.12. *3-Fluoro-4-(4,4,4-trifluorobutyloxy)-4′-heptylbiphenyl (**7**)*

^{1}H NMR ($CDCl_3$) δ: 0.88 (3H, t), 1.30 (8H, m), 1.64 (2H, m), 2.08 (2H, m), 2.36 (2H, m), 2.64 (2H, t), 4.10 (2H, t), 7.00 (1H, m), 7.26 (4H, m), 7.43 (2H, m). IR (KBr)ν_{max}/cm^{-1}: 2920, 1620, 1510, 1250, 1140, 810. MS m/z: 396 (M^+), 311, 201.

6.2.13. *3-Fluoro-4-[(E)-4,4,4-trifluorobut-2-enyloxy]-4′-heptylbiphenyl (**8**)*

^{1}H NMR ($CDCl_3$) δ: 0.88 (3H, t), 1.32 (8H, m), 1.63 (2H, m), 2.63 (2H, t), 4.67 (2H, m), 6.14 (1H, m), 6.57 (1H, m), 6.99 (1H, m), 7.30 (4H, m), 7.44 (2H, m). IR (KBr)ν_{max}/cm^{-1}: 2920, 1600, 1500, 1310, 1240, 1140, 1030, 960, 820. MS m/z: 394 (M^+), 285, 200.

6.2.14. *4-Butyloxy-4′-pentylbiphenyl (**9**)*

^{1}H NMR ($CDCl_3$) δ: 0.89 (3H, t), 0.97 (3H, t), 1.35 (2H, m), 1.58 (6H, m), 1.85 (2H, m), 2.62 (2H, t), 4.02 (2H, t), 6.94 (2H, m), 7.24 (2H, m), 7.48 (4H, m). IR (KBr)ν_{max}/cm^{-1}: 2920, 1600, 1480, 1440, 1240, 1100, 1000, 810. MS m/z: 296 (M^+), 240, 183.

6.2.15. *4-[(E)-But-2-enyloxy]-4′-pentylbiphenyl (**10**)*

^{1}H NMR ($CDCl_3$) δ: 0.90 (3H, t), 1.35 (4H, m), 1.66 (2H, q), 1.75 (3H, d), 2.62 (2H, t), 4.48 (2H, d), 5.67-5.98 (2H, m), 6.96 (2H, d), 7.24 (2H, t), 7.47 (4H, t). IR (KBr)ν_{max}/cm^{-1}: 2920, 2860, 1600, 1500, 1450, 1380, 1250, 1150, 1000, 970, 810. MS m/z: 294 (M^+), 240, 183.

6.2.16. *4-Pentyl-4″-(4,4,4-trifluorobutyloxy)terphenyl (**13**)*

^{1}H NMR ($CDCl_3$) δ: 0.91 (3H, t), 1.36 (4H, m), 1.66 (2H, m), 2.09 (2H, m), 2.35 (2H, m), 2.65 (2H, t), 4.07 (2H, t), 6.98 (2H, m), 7.25 (2H, m), 7.59 (8H, m). IR (KBr)ν_{max}/cm^{-1}: 2930, 1500, 1390, 1250, 1150, 1030, 910, 810. MS m/z: 426 (M^+), 369, 230.

6.2.17. *4-Propyl-4′-(4,4,4-trifluorobutyloxy)tolane (**14**)*

^{1}H NMR ($CDCl_3$) δ: 0.94 (3H, t), 1.65 (2H, sex), 2.06 (2H, m), 2.32 (2H, m), 2.59 (2H, t), 4.03 (2H, t), 6.85 (2H, m), 7.14 (2H, m), 7.43 (4H, m). IR (KBr)ν_{max}/cm^{-1}: 2960, 1600, 1520, 1450, 1250, 1160, 1020, 840. MS m/z: 346 (M^+), 317, 207.

6.2.18. *4-Pentyl-4′-(4,4,4-trifluorobutyloxy)tolane (**15**)*

^{1}H NMR ($CDCl_3$) δ: 0.89 (3H, t), 1.31 (4H, m), 1.57 (2H, m), 2.07 (2H, m), 2.32 (2H, m), 2.60 (2H, t), 4.03 (2H, t), 6.85 (2H, m), 7.14 (2H, m), 7.44 (4H, m). IR (KBr)ν_{max}/cm^{-1}: 2920, 1600, 1520, 1250, 1160, 1025, 835. MS m/z: 374 (M^+), 317, 207.

6.2.19. *4-Heptyl-4′-(4,4,4-trifluorobutyloxy)tolane (**16**)*

^{1}H NMR ($CDCl_3$) δ: 0.81 (3H, t), 1.22 (8H, m), 1.53 (2H, m), 2.00 (2H, m), 2.26 (2H, m), 2.53 (2H, t), 3.96 (2H, t), 6.78 (2H, m), 7.07 (2H, m), 7.36 (4H, m). IR (KBr)ν_{max}/cm^{-1}: 2930, 1630, 1520, 1250, 1150, 1025, 830. MS m/z: 402 (M^+), 317, 207.

6.2.20. *4-Propyl-4′-[(E)-4,4,4-trifluorobut-2-enyloxy]-tolane (**17**)*

^{1}H NMR (CDCl$_3$) δ: 0.94 (3H, t), 1.64 (2H, sex), 2.60 (2H, t), 4.67 (2H, m), 6.08 (1H, m), 6.56 (1H, m), 6.89 (2H, m), 7.14 (2H, m), 7.46 (4H, m). IR (KBr)$\nu_{\max}$/cm^{-1}: 2930, 1610, 1520, 1320, 1240, 1120, 1025, 960, 840. MS *m*/*z*: 344 (M^{+}), 235, 206.

6.2.21. *4-Pentyl-4′-[(E)-4,4,4-trifluorobut-2-enyloxy]-tolane (**18**)*

^{1}H NMR (CDCl$_3$) δ: 0.89 (3H, t), 1.33 (4H, m), 1.61 (2H, m), 2.61 (2H, t), 4.67 (2H, m), 6.06 (1H, m), 6.57 (1H, m), 6.88 (2H, m), 7.15 (2H, m), 7.46 (4H, m). IR (KBr)$\nu_{\max}$/cm^{-1}: 2930, 1600, 1520, 1320, 1240, 1120, 1030, 960, 840. MS *m*/*z*: 372 (M^{+}), 263, 206.

6.2.22. *4-Heptyl-4′-[(E)-4,4,4-trifluorobut-2-enyloxy]-tolane (**19**)*

^{1}H NMR (CDCl$_3$) δ: 0.88 (3H, t), 1.30 (8H, m), 1.61 (2H, m), 2.61 (2H, t), 4.67 (2H, m), 6.07 (1H, m), 6.56 (1H, m), 6.88 (2H, m), 7.14 (2H, m), 7.46 (4H, m). IR (KBr)$\nu_{\max}$/cm^{-1}: 2920, 1610, 1520, 1310, 1250, 1130, 1025, 960, 830. MS *m*/*z*: 400 (M^{+}), 291, 206.

6.2.23. *4-Butyloxy-4″-pentylterphenyl (**20**)*

^{1}H NMR (CDCl$_3$) δ: 0.91 (3H, t), 0.99 (3H, t), 1.37 (4H, m), 1.51 (2H, m), 1.67 (2H, m), 1.80 (2H, m), 2.65 (2H, t), 4.01 (2H, t), 6.98 (2H, m), 7.27 (2H, m), 7.58 (8H, m). IR (KBr)$\nu_{\max}$/cm^{-1}: 2920, 1650, 1570, 1460, 1220, 1100, 1080, 760. MS *m*/*z*: 372 (M^{+}), 315, 259, 230.

6.2.24. *4-[(E)-But-2-enyloxy]-4″-pentylterphenyl (**21**)*

^{1}H NMR (CDCl$_3$) δ: 0.91 (3H, t), 1.36 (6H, m), 1.68 (2H, m), 1.78 (3H, m), 4.51 (2H, t), 5.78 (1H, m), 5.90 (1H, m), 7.00 (2H, m), 7.26 (2H, m), 7.58 (8H, m). IR (KBr)$\nu_{\max}$/cm^{-1}: 2920, 1600, 1500, 1450, 1250, 1150, 1000, 970, 820. MS *m*/*z*: 370 (M^{+}), 315, 259.

6.2.25. *4-Pentyl-4″-[(E)-4,4,4-trifluorobut-2-enyloxy]-terphenyl (**22**)*

^{1}H NMR (CDCl$_3$) δ: 0.90 (3H, t), 1.37 (4H, m), 1.65 (2H, m), 2.65 (2H, t), 4.70 (2H, m), 6.15 (1H, m), 6.60 (1H, m), 7.02 (2H, m), 7.27 (2H, m), 7.60 (8H, m). IR (KBr)$\nu_{\max}$/cm^{-1}: 2920, 1220, 1110, 910, 760. MS *m*/*z*: 424 (M^{+}), 315, 258.

7. Conclusions

The presence of a *trans*-carbon–carbon double bond in the (*E*)-4,4,4-tribut-2-enyloxy chain usually promotes smectic phase formation and leads to higher transition temperatures in general. It also increases the overall dipole moment of these materials due to the elimination of non-linear conformations. The presence of a fluorine atom *ortho* to the terminal chain gives rise to a lower clearing point and suppresses smectic B phase formation probably due to the steric effect of the fluorine atom giving rise to reduced intermolecular attractions. It also increases the dipole moment parallel to the molecular long axis due to additive effects. The extrapolated nematic–isotropic transition temperatures of these materials are relatively high for compounds with two phenyl rings. The tolanes exhibit higher nematic clearing points due to a greater length-to-breadth ratio and a greater anisotropy of polarizability.

Mrs B. Worthington, Mr A. Roberts and Mr A. Rendell are thanked for provision of analytical services. DERA (Malvern) is thanked for financial support of a postgraduate studentship (GWS). The EPSRC is thanked for support of an Advanced Fellowship (SMK). This paper is reproduced with the permission of Her Britannic Majesty's Stationary Office.

References

[1] Schadt, M., and Helfrich, W., 1971, *Appl. Phys. Lett.*, **18,** 127.
[2] Schadt, M., 1997, *Annu. Rev. mater. Sci.*, **27,** 305.
[3] Gooch, C. H., and Tarry, H. A., 1974, *Electron. Lett.*, **10,** 2.
[4] Pohl, L., Weber, G., Eidenschink, R., Baur, G., and Fehrenbach, W., 1981, *Appl. Phys. Lett.*, **38,** 497.
[5] Baur, G., 1981, *Mol. Cryst. liq. Cryst.*, **63,** 45.
[6] Lechner, B. J., 1971, *Proc. IEEE*, **59,** 1566.
[7] Castelbury, D. E., 1979, *IEEE Trans. electron. Dev.*, **ED-26,** 1123.
[8] Dixon, D., 1973, *IEEE Trans. electron. Dev.*, **ED-20,** 995.
[9] Brody, T. P., Asars, J. T., and Dixon, G. D., 1973, *IEEE Trans. electron. Dev.*, **ED-20,** 995.
[10] Howard, W. E., 1986, *Proc. SID '86*, 313.
[11] Morozumi, S., Ohta, T., Araki, R., Kubota, K., Ono, Y., Nakazawa, T., and Ohara, H., 1983, *Japan Display '83*, 404.
[12] Kobayashi, S., Hori, H., and Tanaka, Y., 1997, in *Handbook of Liquid Crystal Research*, edited by Collings, P. J., and Patel, J. S. (Oxford: Oxford University Press).
[13] Kiefer, R., Weber, B., Windscheid F., and Baur, G., 1992, *Japan Display '92*, 547.
[14] Baur, G., 1993, in Proceedings of the 22nd Freiburger Arbeistagung Flüssigkristalle, Freiburg, Germany.
[15] Baur, G., 1994, in Proceedings of the 23rd Freiburger Arbeistagung Flüssigkristalle, Freiburg, Germany.
[16] Baur, G., Kamm, M., Kiefer, R., Klaussman, H., Weber, B., Weber, B., and Windscheid, F., 1994, in Proceedings of the 23rd Freiburger Arbeistagung Flüssigkristalle, Freiburg, Germany.
[17] Gray, G. W., and Kelly, S. M., 1999, *J. mater. Chem.*, **9,** 2037.
[18] Takatsu, H., Takeuchi, K., and Sato, H., 1983, *Mol. Cryst. liq. Cryst.*, **100,** 345.
[19] Gray, G. W., and McDonnell, D. G., 1979, *Mol. Cryst. liq. Cryst.*, **53,** 147.

[20] Eidenschink, R., and Roemer, M., 1983, in Proceedings of the 13th Freiburger Arbeitstagung Flüssigkristalle, Freiburg, Germany.

[21] Finkenzeller, U., Kurmeier, A., and Poetsch, E., 1989, in Proceedings of the 18th Freiburger Arbeitstagung Flüssigkristalle, Freiburg, Germany.

[22] Bartmann, E., Dorsch, D., Finkenzeller, U., Kurmeier, U., and Poetsch, E., 1990, in Proceedings of the 19th Freiburger Arbeitstagung Flüssigkristalle, Freiburg, Germany.

[23] Rieger, B., Poetsch, E., and Reifenrath, V., 1990, in Proceedings of the 19th Freiburger Arbeitstagung Flüssigkristalle, Freiburg, Germany.

[24] Pavluchenko, A. I., Smirnova, N. I., Petrov, V. F., Fialkov, Y. A., Shelyazhenko, S. V., and Yagupolsky, L. M., 1991, *Mol. Cryst. liq. Cryst.*, **209,** 225.

[25] Bartmann, E., Dorsch, D., and Finkenzeller, U., 1991, *Mol. Cryst. liq. Cryst.*, **204,** 77.

[26] Goto, Y., Ogawa, T., Sawada, S., and Sugimori, S., 1991, *Mol. Cryst. liq. Cryst.*, **209,** 1.

[27] Onji, Y., Ushioda, M., Matsui, S., Kondo, T., and Goto, Y., 1993, Eur. Pat. Appl. EPA 0 647 696 A1.

[28] Tarumi, K., Bremer, M., and Geelhaar, T., 1997, *Annu. Rev. mater. Sci.*, **27,** 423.

[29] Takatsu, H., Takeuchi, K., Sasaki, M., and Onishi, H., 1991, *Mol. Cryst. liq. Cryst.*, **206,** 159.

[30] Bartmann, E., Krause, J., and Tarumi, K., 1994, in Proceedings of the 23rd Freiburger Arbeitstagung Flüssigkristalle, Freiburg, Germany.

[31] Bremer, M., 1995, *Adv. Mater.*, **7,** 867.

[32] Reiffenrath, V., Plach, H., Pauluth, D., Hittich, R., Geelhaar, T., Weber, G., and Bartmann, E., 1994, Ger. Pat. Appl. DE 42 22 371.

[33] Plach, H., Bartmann, E., and Pauluth, D., 1995, Ger. Pat. Appl. DE 44 15 882.

[34] Kabalka, G. W., Varma, M., and Varma, R. S., 1986, *J. org Chem.*, **51,** 2386.

[35] Kelly, S. M., Germann, A., and Schadt, M., 1994, *Liq. Cryst.*, **16,** 67.

[36] Suzuki, A., Miyaura, N., and Yanagi, T., 1981, *Synth. Comm.*, **11,** 513.

[37] Buechi, G., and Weinreb, S. M., 1971, *J. Am. chem. Soc.*, **93,** 746.

[38] Skelton, G. W., Brett, P., Jones, J. C., Kelly, S. M., Minter, V., and Tuffin, R. P., *Liq. Cryst.* (submitted).

[39] Petrzilka, M., 1984, *Mol. Cryst. liq. Cryst.*, **111,** 329.

[40] Petrzilka, M., and Schadt, M., 1985, *Mol. Cryst. liq. Cryst.*, **131,** 109.